Colloid Polym Sci 274:555–567 (1996)

ORIGINAL CONTRIBUTION

O. Spalla
M. Nabavi
J. Minter
B. Cabane

Osmotic compression of mixtures of polymers and particles

Received: 12 January 1995
Accepted: 23 November 1995

This work used the x-ray beams of LURE

Dr. O. Spalla (✉) · Dr. B. Cabane
Equipe mixte C.E.A.-R.P.
Service de Chimie Moléculaire
Bât. 125, C.E. Saclay
91191 Gif sur Yvette, France

Dr. M. Nabavi
Equipe mixte C.E.A.-R.P.
Rhone Poulenc
52, rue de la Haie-Coq.
93308 Aubervilliers, France

Dr. J. Minter
Analytical Technology Division
Eastman Kodak, Rochester
New York 14652-3712, USA

Abstract Aqueous dispersions of nanometric ceria particles have been concentrated through osmotic stress. Mixed dispersions of ceria with small adsorbing macromolecules of poly (vinylpyrrolidone) have been prepared by the same method. The osmotic pressure of pure ceria dispersions results from electrostatic repulsions between particles. The osmotic pressure of dispersions containing a non-saturating amount of PVP is the same as that of pure dispersions, and the colloidal stability is depressed with respect to the pure dispersions. The osmotic pressure of dispersions containing an excess of PVP is increased by the free macromolecules, and the colloidal stability is enhanced. The organization of particles in these dispersions has been examined by small-angle x-ray scattering and cryotransmission electron microscopy. In pure ceria dispersions and in saturated dispersions, a liquid-like short-range order was found; when the concentration is increased, this short-range order follows a three-dimensional swelling law. In dispersions containing a non-saturating amount of PVP, the structure shows an alternance of clusters and voids, and the separations of clusters follow an unusual one-dimensional swelling law.

Key words Nanometric particles – osmotic compression – microphase separation

Introduction

Adsorbed macromolecules may be used as "bumpers" or as "stickers" to control interactions between colloidal particles dispersed in a liquid [1–11]. "Bumper" action is obtained when the particle surfaces are saturated with polymer and kept apart by the crowding of polymer segments between them. "Sticker" action is obtained when the particle surfaces are unsaturated and tend to share the available polymer.

However this picture is a simplification of a vastly complicated problem. This problem is made of two parts: the configurations of adsorbed macromolecules, and the effect of these macromolecules on the relative locations of the particles. The first part, macromolecules on surfaces, has been extensively studied and is reasonably well understood [12–15]. The second part, the relative locations of particles, is more difficult.

The main complications result from irreversible adsorption of the macromolecules onto the particles. This may cause heterogeneous coverage [2] or irreversible bridging [3]. A particular procedure for bringing particles and macromolecules together may cause the formation of clusters whereas the state of lowest free energy would be isolated particles [2]. This procedure may also cause the formation of irregular bushy clusters where the clusters of lowest free energy would be dense [5, 6].

There are cases where the adsorption is reversible, and these give more reproducible structures. Reversible

adsorption is more easily obtained when the particles are quite small, because the total adsorption free energy per particle is less. In aqueous systems, two situations with very small particles have been studied; silica particles with adsorbed poly (ethylene oxide) in water at high pH [7, 8], and ceria particles with adsorbed poly (acrylamide) in water at low pH [9, 10]. In both systems, however, the macromolecules are much larger (40–100 nm) than the particles (4–20 nm); consequently each macromolecules can bind many particles in a row. These necklace structures complicate the analysis, because there is no simple interparticle potential energy that can reproduce the interactions within a necklace and between necklaces.

In the present work we chose a colloidal system where both complications are eliminated. Particles and polymers are of comparable sizes, both quite small (4–10 nm). Furthermore they interact weakly with each other. Consequently, each macromolecules has few bound monomers and the total binding energy per macromolecule is low.

We report the results of experiments in two regimes: the dilute regime, where each particle interacts with one other particle only, and the concentrated regime, where it interacts with many others. These measurements have been performed on the pure dispersions, on dispersions with an amount of polymer which does not saturate the surfaces, and with a saturating amount of polymer.

In the dilute regime, we have studied the extent of association between all particles and macromolecules in the dispersions. First we have measured the binding of macromolecules to particles by separating bound and unbound macromolecules. Second, we have determined the limits of colloidal stability for dispersions with different amounts of adsorbed macromolecules. Third, we have determined the number of independent objects in each dispersion from measurements of its osmotic pressure.

In the concentrated regime, we have studied the effect of the macromolecules on the relative locations of particles in the dispersions. First, we measured the resistance of the dispersions to osmotic compression. Second, we have determined the structures of the dispersions through small-angle x-ray scattering (SAXS) and through fast freezing electron microscopy. These results characterize the effect of polymers as a potential acting on interparticle distances, which is a formal way of describing the "bumper" or "sticker" effect of polymers in the colloidal dispersion.

Materials

Ceria particles

Nanometric ceria particles can be obtained through precipitation in aqueous solutions of $Ce^{4+}(NO_3^-)_4$ and HNO_3 [16]. The composition of the precipitate is:

$$CeO_2(HNO_3)_{0.5}(H_2O)_4 \,. \qquad (1)$$

Addition of water to this precipitate causes it to redisperse into a colloidal sol. The dispersion contains nanometric particles, which have been characterized through a variety of techniques. X-ray diffraction of precipitates and of peptized sols yields broad diffraction lines, which match the lines of ceria [17]. Electron microscopy pictures of dried dispersions also show crystalline particles [17]. The weight average mass per particle was determined from static light scattering; it is $M_w = 2*10^5$ g/mole [9]. The hydrodynamic diameter of the particles was determined from quasielastic light scattering; it is 60 Å [9].

The number average mass M_n of ceria per particle has been determined in this work through two different methods. Osmotic pressure of dilute dispersions of ceria yields $M_n = 1.4*10^5 \pm 0.2*10^5$ g/mole. Interparticle distances measured through SAXS in concentrated dispersion yield $M_n = 1.5*10^5 \pm 0.2*10^5$ g/mole.

These particles have a very large surface area: from the Porod limit in SAXS we have obtained $A = 400\ m^2/g$, or $93\ nm^2$/particle. This surface is covered with hydroxyls and covalently bound nitrates [18]. In water at low pH some of the hydroxyls are protonated; there are about 200 positive charges per particle at pH 2, which are compensated by nitrate anions in the Stern and diffuse layers surrounding each particle.

Aqueous dispersions

Dispersions of the precipitate in water give colloidal solutions which contain high concentrations of nitric acid and low concentrations of other ions, mainly Ce^{III} cations or polycations. These ions were removed through dialysis against aqueous nitric acid solutions. The final pH of the dispersion can be set in the range 0.5 to 3. All dispersions in this work were prepared at pH 2.

The resulting dispersions have colloidal stability if the ionic strength is below 0.55 M and the pH is below 2.5. The reasons for this limited range of stability have been explained [18]. At higher ionic strength the electrostatic repulsions between particles are screened by the high concentration of anions, and Van der Waals attractions cause the particles to flocculate; this flocculation is reversible because the surfaces are protected by the covalently bound nitrates. At higher pH the covalently bound nitrates are replaced with hydroxyls, and the ceria surfaces become reactive towards each other; electrostatic repulsions are not sufficient to keep them apart at all times; consequently the particles aggregate. This aggregation is not reversible.

Polymers

Poly (vinyl pyrrolidone), hereafter abbreviated PVP, was bought from FLUKA. The macromolecules were characterized through size exclusion chromatography in water. The use of a light scattering detector together with a differential refractometer gave an absolute determination for the molar mass of the eluted fractions. For this polymer, we obtained $M_w = 35\,000$ and $M_n = 14\,000$, which yields $M_w/M_n = 2.5$.

Water is a good solvent for these polymers. In our experiments the polymers were dissolved in aqueous HNO_3 solutions at pH 2. In dilute solutions, the macromolecules are well separated; their hydrodynamic radius is 100 Å. In concentrated solutions they are forced to overlap; the overlap concentration can be estimated by static light-scattering experiments. A plot of scattered intensity versus concentration has a maximum which corresponds to the onset of strong interactions between the macromolecules [19]; this is the overlap concentration c^*. In our case, $c^* = 50$ g/l.

PVP macromolecules are soluble in water because the carbonyl group is strongly solvated by water molecules. Through this large dipole they also interact with polar surfaces. The interaction of PVP with ceria originates from an attraction between the carbonyls on PVP and the OH of the surface hydroxyls [20].

Methods

Osmotic pressure measurements

The osmotic stress method was used to equilibrate the content of the dispersions according to osmotic pressure, pH and ionic strength. The principles of osmotic stress were established by Parsegian et al. [21] and by Rohrsetzer et al. [22]. This method is based upon exchanges of water and salt between the sample and a reservoir, through a membrane that is permeable to salt and water. The osmotic pressure in the reservoir is set by a water soluble polymer. The polymer used in this work (dextran) is not preferentially solvated by most salts. Consequently, its osmotic pressure is related to its concentration only. The chemical potential of the salt in the sample is set by the salt concentration in the reservoir.

Two types of dextran, obtained from FLUKA, were used in this work; the molar masses given by the manufacturer were 70 000 and 110 000 g/mole. The distributions of molar mass were checked through size exclusion chromatography (SEC); they were found to be monomodal with a polydispersity index $M_w/M_n = 2.1$ for the 70 000 grade and $M_w/M_n = 1.6$ for the 110 000 grade. The average molar masses found by SEC were 71 000 g/mole and 110 000 g/mole.

The osmotic pressures of dilute dextran solutions in water at pH 2 were measured with a KNAUER membrane osmometer up to a weight fraction 5%. For the Dextran grade 70 000 the results were fitted by a polynomial expression for pressure Π in pascals versus concentration c in weight %.

$$\Pi = -16.24 + 345.05c + 79.50c^2 + 7.12c^3. \quad (2)$$

The dextran grade 70 000 was used in the range of concentration below 5%; thus Eq. (2) was be used to calculate the osmotic pressure.

In the case of dextran grade 110 000, additional measurements were done as follows. The osmotic pressure was calculated by Cécile Roselli in the range of 2–15% using the integration of static light scattering intensities versus concentration. In the range 16% to 35%, measurements were made by Cécile Bonnet-Gonnet using a vapor pressure osmometer. All results concerning dextran grade 110 000 were fitted by the following equations which also match the fits proposed by Parsegian et al. [23] (Π is given in dyne/cm^2):

$$\mathrm{Log}(\Pi) = 1.385 + 2.185c^{0.2436} \quad C \leq 10\% \quad (3)$$

$$\mathrm{Log}(\Pi) = 1.872 + 1.657c^{0.3048} \quad C \geq 10\% \,. \quad (4)$$

Ceria dispersions were placed in dialysis bags which allowed exchange of water and ions but not of PVP or particles; this was obtained with a cut-off at a molar mass of 12 000. These bags were immersed in the stressing solutions of dextran at pH 2. During the initial deswelling of the dispersions it was necessary to refill the bags and to exchange the stressing solutions; equilibrium was reached after 3 weeks.

The ceria concentration in each dialysis bag was determined by chemical titration: the ceria was dissolved in concentrated sulfuric acid in the presence of phosphates, the resulting Ce^{4+} ions were reduced to Ce^{3+} by a known amount of Fe^{2+} (Mohr salt), and the excess Fe^{2+} was titrated with a solution of potassium bichromate. The concentration of dextran in the reservoir was measured through carbon analysis; from this concentration the osmotic pressure was calculated according to expressions (2) or (3) and (4).

Cryo-transmission electron microscopy

Thin vitrified specimens were prepared for transmission electron microscopy in a controlled environment vitrification system (CEVS), at fixed temperature and 100%

Colloid & Polymer Science, Vol. 274, No. 6 (1996)

relative humidity. This assured minimal changes in the specimen prior to vitrification. Thin liquid films were prepared on perforated carbon films supported on 3 mm electron microscope grids. A specimen was prepared by applying a small (about 3 μl) drop onto the grid, blotting most of it to the desired thickness (under 200 nm) and plunging it into liquid ethane at its melting point. This ultra-fast cooling caused vitrification of the liquid phase, i.e., specimens became solid-like (vitreous) without change of phase that leads to microstructural rearrangement. These cryo-specimens were stored under liquid nitrogen, and transferred to the cooling-holder (Gatan 626) of the TEM (JEOL 2000FX), where they were equilibrated at $-170\,^{\circ}C$, and examined with an acceleration voltage of 100 kV. More details about the technique are given in refs. [24–29].

Small-angle x-ray scattering

The structures of dispersions were investigated through SAXS. Experiments were performed on the instrument D22 of LURE [30]. X-rays of wavelength 1.15 Å were selected through a crystal monochromator and directed on the sample through a system of slits with point collimation; scattered rays were collected with a linear counter at a distance of 0.565 m. Scattered intensities were measured according to the scattering vector Q; the complete range of Q was from $Q = 0.012\,\text{Å}^{-1}$ (distance ≈ 500 Å) to $Q = 0.4\,\text{Å}^{-1}$ (distance ≈ 15 Å).

Scattering is produced by heterogeneities in the sample, which must be regions where the electron density is either higher or lower than average. These heterogeneities may be particles or aggregates of particles, because the electron density of ceria is much higher than that of water. Organic polymers such as PVP contribute little to the scattering because their electron density is close to that of water.

The intensity scattered by a dispersion of identical particles can be expressed as a product of the form factor $P(Q)$ which describes interferences between rays scattered by atoms within a particle, and the structure factor $S(Q)$ which describes interferences between rays scattered by atoms located in different particles [31]:

$$I(Q) = P(Q)S(Q)\,. \tag{5}$$

The experimental form factor $P(Q)$ was obtained in dilute regime (below 0.002%) where $S(Q) \approx 1$. Assuming for simplicity a monodisperse distribution of shapes and sizes, the best fit was obtained with a flat ellipsoid of diameters $\sigma_1 = \sigma_2 = 70$ Å and $\sigma_3 = 14$ Å. This leads to a volume $V = 36\,000$ Å^3 and a mass $M = 1.54{*}10^5$ g/mole. These values are in close agreement with the osmotic pressure determination of the mass per particle.

The structure factor $S(Q)$ is the Fourier transform of the pair correlation function $g(r)$ of particles. If the particles repel each other, then there is around each particle a forbidden region which no other particle may enter; accordingly $g(r)$ is near zero at low r, and rises to unity beyond the diameter of the forbidden region. This depression produces an oscillation in $S(Q)$ [31, 32]. Strong repulsions result in a short-range order for the particles, which produces a maximum in $g(r)$ at the average interparticle distance; then the oscillation in $S(Q)$ turns into a peak from which the average interparticle distance may be calculated [33].

Results

Adsorption

The addition of PVP macromolecules to ceria dispersions at pH 2 without added salt did not cause phase separation. Consequently, in order to measure the adsorbed amount, it was necessary to separate the polymer covered particles through centrifugation. Three adsorption isotherms were determined at adsorbent concentrations 2 g/l, 6 g/l and 10 g/l; they are shown in Fig. 1. There is some uncertainty in the value of the specific area of ceria particles, therefore the data are presented as an adsorbed amount per weight of ceria. They present some common features which can be compared to classical theories of polymer adsorption:

i) At low concentration of free polymer there is a linear rise of the adsorbed amount with increasing concentration of free polymer. The linear regime is steeper when the adsorbent dispersion is less concentrated.

ii) At high concentration of free polymer there is an apparent saturation of the bound amount of polymer. For different adsorbent concentrations, this apparent saturation occurs at different levels of coverage. However, we have explored only a limited range of free polymer concentration. Consequently the apparent saturation may not be complete; in the following it will be called "pseudo-saturation".

The first feature is opposite to the behaviour of strongly adsorbed polymers. Indeed, in this limit, Scheutjens and Fleer [15] have shown that the isotherm should not have a linear increase at low concentration. A linear rise can be observed only if the polymer is very short (less than 25 monomers) or if the adsorption is very week (much less than kT per monomer). Both reasons may apply here. First, the polymers are short (140 monomers per macromolecule). Second, they compete for adsorption sites with

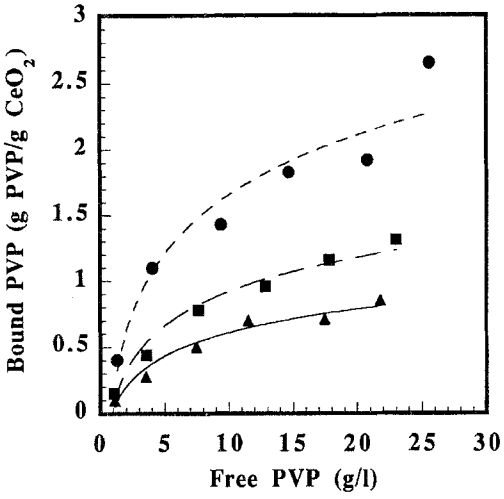

Fig. 1 Adsorption isotherms for the binding of PVP to the surfaces of ceria particles at pH 2. Horizontal axis: concentration of free PVP, in g/l. Vertical axis: amount of PVP bound to the particles, in g of PVP per g of ceria. The plateau of the isotherm depends on the concentration of ceria. ▲: 10 g/l ceria; ■: 6 g/l of ceria; ●: 2 g/l of ceria

nitrates ions [18]; therefore the net adsorption enthalpy may be quite low. A similar linear rise was observed with a different polymer (PAM) on the same ceria particles [9].

The second feature may originate from the polydispersity of the adsorbing polymer. Indeed, Cohen-Stuart et al. [20, 34] have shown that the polydispersity of the macromolecules induces an increase of the pseudo saturation when the adsorbent dispersion is less concentrated. The theory is based on two assumptions: the plateau of a monodisperse sample increases with the molecular weight of the macromolecule and the large macromolecules adsorb onto the surface preferentially to the smaller ones.

The Cohen-Stuart analysis still yields the classical rounded shape for the adsorption isotherm [20, 34]. In the present case, however, two features must be accounted for: a linear increase at the beginning of the isotherm, and a pseudo-saturation at the end. This combination can be obtained if it is assumed that monodisperse PVP macromolecules have a weak affinity for the particles and that the macromolecules are in fact polydisperse. In that case, the solution contains macromolecules that have different affinities for the particles, with a very weak affinity for the smallest macromolecules.

The mechanism of surface speciation proposed by Cohen-Stuart can explain the general features of the isotherms. When the adsorbent dispersion is dilute (2 g/l), the amount of bound polymer represents a small fraction of the total polymer. This fraction is made of the highest molar masses which adsorb "strongly" on the surface and produces a high apparent plateau. To the contrary, when the adsorbent dispersion is more concentrated (10 g/l), the amount of bound polymer represents a larger fraction of the total polymer, and the average molar mass of this fraction is lower. Hence, the average affinity is weaker and the apparent saturation level is lower.

This weak affinity of the macromolecule for the surfaces has two main consequences: a) the adsorption is reversible and the mixtures are at equilibrium and b) the saturation of the adsorption is reached only at a substantial concentration of free polymer; for instance, in a "pseudosaturated" dispersion containing 10 g/l of ceria, there are seven bound macromolecules and 14 free macromolecules per particle.

For simplicity, we classify all samples according to the mass ratio of total PVP to total ceria; sample with ratios below 2 g/g are considered as "unsaturated", and samples exceeding 2 g/g are considered as "saturated".

Stability of dilute dispersions

In dilute dispersion at pH 2, ceria particles repel each other. These repulsions can be depressed by the addition of passive salt. Beyond a critical ionic strength, called the Critical Coagulation Concentration (ccc), the interactions become attractive and the particles aggregate as fast as their diffusive motions allow. The ccc is a good measure of the strength of repulsive interactions in a dispersion; for a ceria dispersion at pH 2, the ccc is reached after adding 0.55M of $NaNO_3$.

The addition of PVP alters these interactions; this effect can be quantified by measuring the variation of the ccc according to the adsorbed amount of PVP. Figure 2 shows these variations for a dispersion at 10 g/l of ceria. The addition of small amounts of PVP (less than 2 g/g ceria) lowers the ccc of the dispersion compared with the pure ceria dispersion. Accordingly, small amounts of polymer have a destabilizing effect on the dispersion. This effect is reversed at high concentrations of PVP, where more salt is required to initiate the coagulation. Accordingly, the addition of large amounts of PVP can *stabilize* the dispersions and prevent their coagulation at high ionic strengths. This steric stabilization is observed in many other systems [35].

The reversal occurs at a total PVP concentration of 1.8 g of PVP per g of ceria. Remarkably, this is also the amount of PVP which is required to "pseudo" saturate the particle's surface (Fig. 1). Thus it may be concluded that particles with *unsaturated surfaces* bind to each other more easily than bare ceria particles, whereas particles with *saturated surfaces* are prevented from binding altogether.

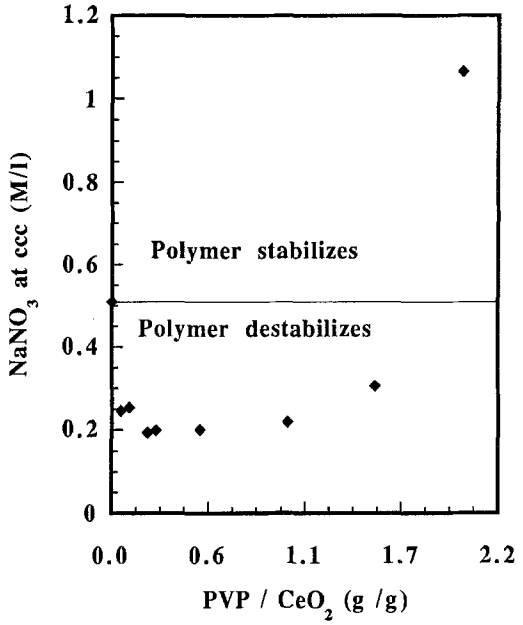

Fig. 2 Critical coagulation concentration of dispersions at pH 2, with 10 g/l of ceria and increasing amounts of polymer. Horizontal axis: amount of added PVP, in g of PVP per g of ceria. Vertical axis: concentration of $NaNO_3$ required to obtain fast coagulation of the dispersion, in mol/l

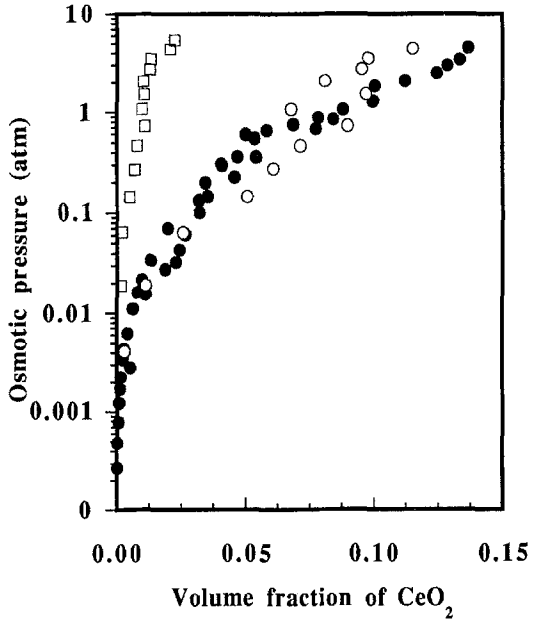

Fig. 3 Osmotic pressures of ceria dispersions. Horizontal scale: volume fraction of ceria in the dispersion. Vertical scale: osmotic pressure, in atmospheres. •: pure ceria dispersions. ○: ceria + PVP with unsaturated surfaces. □: ceria + PVP with saturated surfaces

Osmotic pressure

In concentrated dispersions, the repulsions between particles are measured through the resistance of the dispersion to an osmotic stress. The experiment measures the concentration of the dispersion resulting from this stress, and the data are presented as an equation of state, i.e. a curve of osmotic pressure Π vs. volume fraction of ceria. In this section, equations of state are presented for pure ceria dispersions, and for dispersions of ceria with added PVP.

Pure ceria dispersions

The equation of state for pure ceria dispersions is presented in Fig. 3. For a dispersion of separate objects the pressure has the general form:

$$\Pi = \rho kT f(\Phi) \tag{6}$$

where ρ is the number density of objects and $f(\Phi)$ is the osmotic coefficient which measures the deviation from ideality due to interactions between the particles. For a colloidal dispersion, $f(\Phi)$ tends to unity when Φ tends to zero, provided that the dilution is done with a background of electrolyte. Then, in the high dilution limit, Eq. (6) can be rewritten as follows:

$$\Pi/(ckT) = N_A/M_n \,, \tag{7}$$

where c is the concentration of particles (g/l). Hence, in a first step, Eq. (7) is used to deduce the mass per particle M_n; it yields $M_n = 1.4{*}10^5 \pm 0.2\,10^5$ g/mole. Then, as the volume fraction increases, the pressure deviates from the perfect gas law due to interparticle repulsions. Hence, the osmotic coefficient $f(\Phi)$ becomes much greater than unity as shown in Fig. 4.

At volume fraction $\Phi < 0.01\%$, the strength of repulsion is measured by the initial slope in Fig. 4 which gives the second coefficient b of the virial expansion:

$$f(\Phi) = 1 + b\rho \,. \tag{8}$$

If we assume that the particles behave like effective hard spheres because of their double layer repulsions, then b is related to the effective particle volume through:

$$f(\Phi) = 1 + 4\Phi_{\text{eff}} \,. \tag{9}$$

The experimental slope yields to $\Phi_{\text{eff}} = 30\,\Phi$, which corresponds to an effective diameter three times larger than that of the hard sphere case. For $M_n = 140\,000$ g/mole one obtains a hard-sphere diameter $\sigma = 41$ Å and an effective diameter of 125Å. This value is slightly different from the

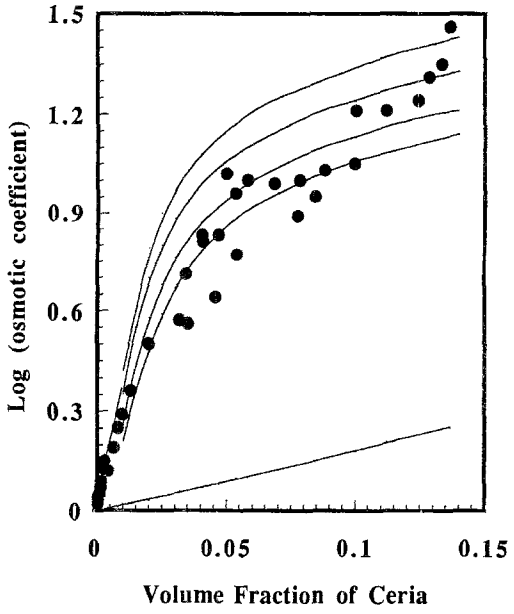

Fig. 4 Osmotic coefficient of pure ceria dispersion in semi-log representation. The slope at zero concentration gives the second virial coefficient. The lowest continuous line corresponds to the Carnaham-Starling equation for pure hard sphere and shows that the pressure is entirely dominated by the electrostatic interactions. Other lines correspond to PB-Cell in osmotic equilibrium and constant charge. The charge per particle is, from bottom to top $Z = 20, 27, 50, 200$

one (140 Å) obtained by measuring the second virial coefficient with light scattering [9]; the difference originates from the polydispersity ($M_w/M_n = 1.4$).

The measured second virial coefficient b can be compared with a calculation of interparticle repulsions:

$$b_{th} = \int_0^{+\infty} 1 - e^{-\beta U(r)} dr \tag{10}$$

where the pair potential $U(r)$ is calculated from DLVO theory [36] according to the values of the effective charge Z_{eff} per particle and of the screening constant κ:

$$\beta U(r) = \frac{Z_{eff}^2 L_b e^{-\kappa(r-\sigma)}}{r(1+\kappa\frac{\sigma}{2})^2}. \tag{11}$$

At low volume fractions, κ may be calculated directly from the concentration of free protons and nitrates in the dispersion ($I = 0.01$ M at pH2). Then b_{th} depends on Z_{eff} only. Setting $b_{th} = b_{exp}$ yields $Z_{eff} = 16$. This value matches the classical criterium of effective charge, $Z_{eff}L_b/2\sigma = 1$ [37].

When the volume fraction is greater than 0.01, the number of counter-ions is no longer negligible and contributes to the ionic strength. Consequently, the effective diameter of the particle depends on the concentration Φ. Then, a more effective way to calculate the electrostatic pressure is to use a PB-cell model. The program that we have used, written by Luc Belloni [38], accounts for the osmotic equilibrium of the ions with a reservoir at a fixed concentration of salt. When the concentration of particles is varied, calculations can be performed either at constant potential, constant charge or constant equilibrium. Calculations were made at a constant charge Z_{PB}; the osmotic pressure curves calculated with different choices of Z_{PB} are shown in Fig. 4. The best fit to the data is obtained with $Z_{PB} = 27$. This value is much below the number of ionizable sites measured through potentiometric titrations [18]. The differences originates from the adsorption of strongly bound counterions, which reduce the number of sites that carry a net charge.

The reverse experiment, reswelling compressed dispersions, was also performed. In a first step, it was limited to samples which had been concentrated to volume fractions up to 0.03. These samples were kept in the dialysis bags and immersed in dilute dextran solutions (3%). After 10 days of equilibration the ceria content of the bags were analyzed. It was found that the samples reswelled back to the volume fractions expected for dispersions in equilibrium with a 3% dextran solution. Hence, the compression of the dispersions was reversible. This experiment demonstrated that no irreversible aggregation of the ceria particles had occurred.

Further reswelling experiments were done on samples which had been concentrated to $\Phi > 0.03$. These samples did not reswell back to their initial volumes. Dilutions of these partially reswelled samples were examined through light scattering; clusters of particles were observed. Hence, we conclude that a partial aggregation had occurred deswelling beyond $\Phi = 0.03$. Nevertheless, in the range of volume fractions $\Phi = 0.03$ to 0.15, the osmotic pressure is still fitted by a model of electrostatic interactions between particles. This suggests that a partial aggregation does not change the contribution of electrostatic interactions to the osmotic pressure.

Dispersions with polymer covered surfaces

For dispersions with added PVP, the osmotic pressures depend on the amount of polymer on the surfaces. A first series of samples was made at a coverage which gives the lowest stability of the dispersions, as measured by the ccc (see above). The composition was 0.2 g of polymer per g of ceria. The second series was made with saturated surfaces, at the coverage (2 g of polymer per g of ceria) which gives increased stability of the dispersion compared with the pure ceria dispersion. The pressures and volume

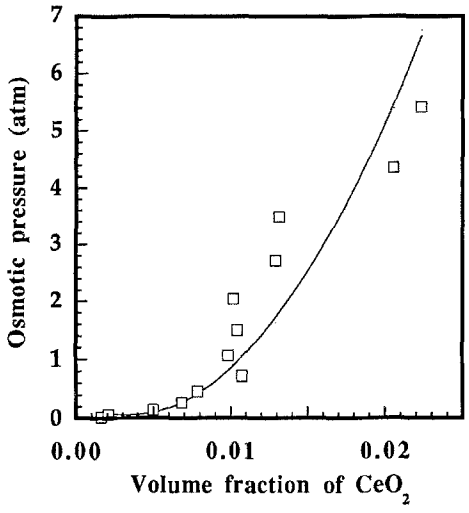

Fig. 5 Osmotic pressures of ceria dispersions saturated with 2 g of PVP per g of ceria (□). The full line corresponds to a fit of the experimental pressures of pure PVP solutions at the same concentration of PVP in the same volume of aqueous solution

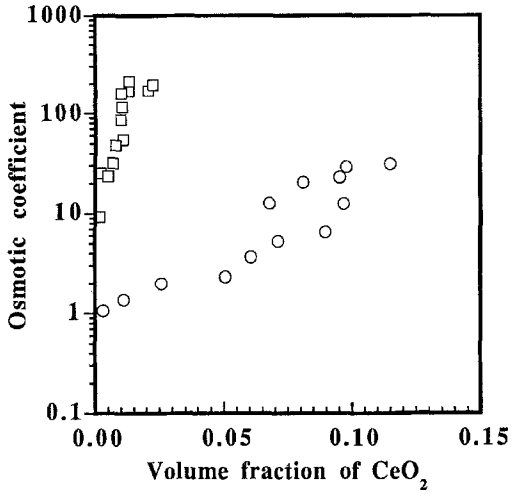

Fig. 6 Osmotic coefficients of ceria dispersions with added PVP. Horizontal scale: volume fraction of ceria in the dispersion. Vertical scale: log(osmotic coefficient). ○: ceria + PVP with unsaturated surfaces. □: ceria + PVP with saturated surfaces

fractions measured for these two series of samples are presented in Fig. 3.

Dispersions made with *saturated surfaces* turned out to be much less compressible than pure ceria dispersions. Further experiments were made in order to determine the origin of this resistance. Indeed, it may originate from the volume of adsorbed polymer layers, or from the volume of free macromolecules, or from both. For this purpose, the pressures and volume fractions of pure PVP solutions were measured and compared with those of ceria + PVP dispersions at the same concentration of PVP in the aqueous solution. The comparison (Fig. 5) shows that the pressures of free PVP solutions match those of dispersions saturated with PVP. Thus PVP macromolecules in the saturated dispersions take up volume and resist compression as much as free PVP macromolecules.

The presence of free polymer was confirmed by a calculation of the number N of independent objects in the dispersion. This number may be obtained from the values of Π/kT in the limit of large dilutions. Figure 6 shows the same sets of data plotted as $\Pi/(\rho kT)$. For pure ceria dispersions, this ratio tends to unity at low volume fractions (Fig. 4). For the mixed dispersions with 2 g of PVP per g of ceria, this ratio goes to a limit of 10. Therefore the number of objects in the limit of large dilutions is much larger than the number for particles. It is comparable with the number of macromolecules. Indeed, the ceria concentration of the more dilute point on Fig. 6 is 11 g/l; according to the adsorption isotherm (at 10 g/l) there are seven bound and 14 free macromolecules for each particle. Hence the ratio $\Pi/\rho kT$ should be 15 if the polymer-covered particles and the excess macromolecules behave as independent objects. This prediction is in good agreement with the experimental value.

The compression curve of the dispersion with *unsaturated surfaces* is comparable to that without polymer (Fig. 3). In the dilute limit, the number of independent objects is the same as for the pure ceria dispersion (Fig. 6). This result provides some information about the way particles share the macromolecules in the dilute regime. The number of adsorbed macromolecules is determined using the adsorption isotherm. The first point on the osmotic curve is at a ceria concentration of 21 g/l. Using the isotherm obtained at a ceria concentration of 10 g/l, there are 0.5 free and 1.5 bound macromolecule per particle. Assuming that every bound macromolecule is linked to one particle only, the osmotic coefficient relative to the number of ceria particles ($\Pi/\rho kT$) should be equal to 1.5. The experimental value is very close to 1.5, showing that the bound macromolecules do not bind particles together. The absence of polymer bridges in the dilute regime originates from the small size of the macromolecules. Indeed, the macromolecule should be larger than the effective range of electrostatic repulsions in order to bridge particles together [9].

In the concentrated regime, the osmotic pressures of dispersions with polymer remain close to those of dispersions without polymer. Yet the macromolecules may bridge the particles together, since the interparticle distances are now shorter than the sizes of the macromolecules. The osmotic pressure indicates that such bridges do not

modify the thermodynamic properties of the dispersion. This result is similar to the behavior of pure ceria dispersions, where a partial aggregation of the particles does not change the osmotic pressure. Both results may have a common origin : in electrostatically stabilized dispersions, the osmotic pressure originates from the entropy of counterions [38]. This entropy is determined mainly by the volume accessible to the counterions; thus we may infer that such aggregation processes do not change the volume accessible to the counterions.

Still, other properties of the dispersions may be affected by the presence of macromolecules. In particular, the ordering of the particles (e.g. $S(Q)$ at $Q \sim$ inverse interparticle distances) may be affected even if the osmotic pressure (e.g. $S(Q)$ at $Q = 0$) is unchanged. Results concerning this ordering are presented in the next section.

Structure of concentrated dispersions

Small-angle x-ray scattering

Experiments were performed on dispersions made of pure ceria or ceria + PVP, at pH 2 and ceria volume fractions in the range $\phi = 0.002$ to 0.15. Even though these volume fractions are not large, the number density of particles is high, and the average interparticle distances are short, of the order of 100 Å. In these conditions, all dispersions give a peak in the curve of scattered intensity I versus scattering vector Q; the position of this peak varies with the volume fraction of ceria. Typical scattering curves are shown in Fig. 7.

As explained in "Methods", the peak position is related to the average interparticle distance. Indeed, in a concentrated dispersion, there is a liquid-like order of the particles and $S(Q)$ can be calculated using integral equations [32] where the number of particles, the charge of the particle and the ionic strength are the only parameters. In our procedure, the number of particles is calculated from the concentration assuming a mass M_n for the particle. Thus, the mass M_n and the effective charge Z_{eff} of the particle are the fitting parameters. The ionic strength of the dispersion is calculated by adding contributions from passive salt and from free counterions:

$$2I = 2I_0 + Z_{eff}{}^* \rho \,, \tag{12}$$

where we set I_0 to its values in the reservoir (0.01 mol/l) although we are aware that there is some salt exclusion under osmotic stress. For the more dilute dispersion, the best fits was obtained with $M_n = 1.6\ 10^5$ g/mol and $Z_{eff} = 25$, and for the more concentrated dispersion it was obtained with $M_n = 1.4\ 10^5$ g/mol and $Z_{eff} = 17$ (Fig. 7).

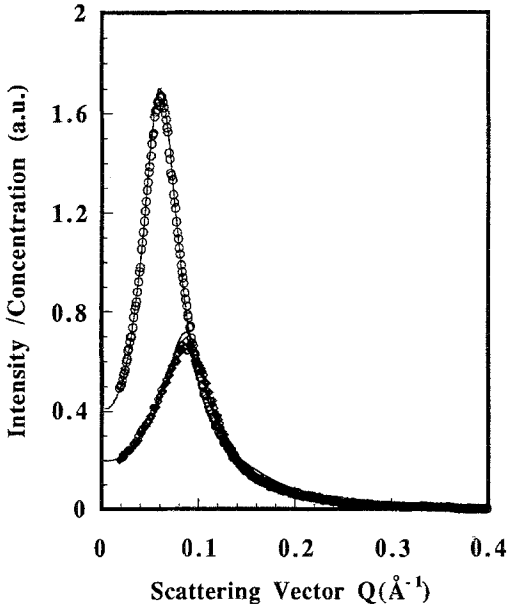

Fig. 7 Small-angle x-ray scattering curves of ceria dispersions. Horizontal scale: scattering vector Q, in $Å^{-1}$. Vertical scale: scattered intensity, in arbitrary units. ○: ceria in aqueous HNO_3 solutions at pH 2, volume fraction of ceria $\phi = 0.023$. ◇: same with a volume fraction $\phi = 0.079$. The peak position is related to the average interparticle distance. The two full lines correspond to liquid order fits described in the text

These values are in good agreement with the ones determined from osmotic pressures.

The complete set of SAXS results, for pure ceria dispersions, shows that the peak position varies as a power law of volume fraction, and the exponent is 1/3 (Fig. 8). This is the swelling law expected for an isometric organization of the particles, where distances in all directions vary in the same way. The coefficient of this swelling law can be used to determine the number of independent particles in concentrated dispersions. For this purpose, we assume that the observed short-range order (SRO) swells in the same way as a regular long-range order (LRO). This is a good approximation when the particles interact through soft repulsive potentials [33]. In the case of a face centered cubic LRO, the relation between peak position, volume fraction and particle size would be:

$$(q_{peak})^3 = (2\pi)^2\, 9\sqrt{3}\, (\sigma)^{-3}\, \phi \,. \tag{13}$$

The straight line in Fig. 8 corresponds to Eq. (13) with $\sigma = 40 \pm 2$ Å. This yields a mass $M_n = 1.5\,10^5 \pm 0.2\ 10^5$ g/mol which is again in good agreement with the osmotic result and confirms the validity of Eq. (13) in our case.

For *dispersions with nearly saturated surfaces* (2 g of PVP per g of ceria), the peak position follows the same

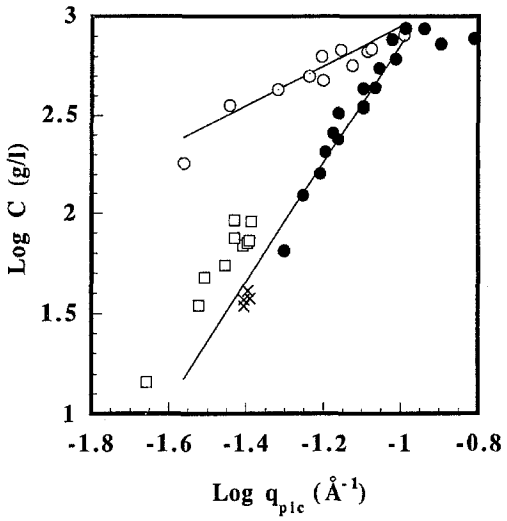

Fig. 8 Positions of the peaks in the small-angle scattering curves. Horizontal scale: $\log_{10}$ (peak position in $Å^{-1}$). Vertical scale: $\log_{10}$ (volume fraction of ceria in the dispersion). ●: pure ceria dispersions. ○: ceria + PVP with unsaturated surfaces. □: ceria + PVP with nearly saturated surfaces (2 g/g). ×: ceria + PVP with fully saturated surfaces (5 g/g). The line of slope 1/3 corresponds to a perfect fcc packing (Eq. (15)) with $M_n = 1.5*10^5$ g/mole

power law with volume fraction; however the peaks are at slightly lower Q values than for pure ceria, indicating larger distances (Fig. 8). This is possible only if the scattering objects are made of more than one particle each; the average number of ceria particles per scattering object is 1.7. This slight aggregation may be due to an incomplete coverage of the surfaces by the polymer. To verify this hypothesis, experiments were performed on dispersions containing 5 g of PVP/g of ceria. For this composition the peak position are located exactly on the swelling law of pure ceria. This confirms that in dispersions containing 2 g PVP/g of ceria the surfaces are not fully protected. The complete protection is reached for higher concentration of polymer.

For *dispersions with unsaturated surfaces* (0.2 g of PVP per g of ceria) the distances follow a different law. As shown in Fig. 8, the dispersion made at $\Phi = 0.11$ gives the same peak position as the pure ceria dispersion; however, at lower volume fractions, these dispersions yield distances which expand much more rapidly than in pure ceria: indeed the exponent is 1 instead of 1/3. Nevertheless, all the spectra have the general shape shown in Fig. 7: the peaks are broad, as expected for a liquid-like order. Since the distances are then much larger than in the pure ceria dispersions, it follows that the scattering objects must be aggregates containing many particles each. The linear law for the variation of the distance between these aggregates must reflect the way in which they separate from each other when more aqueous solution is added, or the way in which they come together when the dispersion is compressed.

At low volume fractions, this swelling law is interrupted. Indeed, osmotic pressure measurements in dilute dispersions indicate that the number of independent objects equals the number of ceria particles. Hence, the aggregates dissemble at large dilution. This makes it impossible to determine the structure of individual aggregates through scattering. For this purpose, we turned to electron microscopy.

Electron microscopy

Images of dispersions made in the middle of the concentration range were obtained through cryo-transmission electron microscopy. These images represent projections onto a plane of a thin concave film of dispersion.

Figure 9 presents an image of a dispersion containing ceria only. The ceria particles appear as small dark grains, with stone-shape and diameters around 5 nm. They are randomly distributed throughout the dispersion; this is consistent with SAXS results which show no preferred

Fig. 9 Image of a dispersion containing 5 g/l ceria in aqueous HNO_3 at pH 2, obtained through cyo-transmission electron microscopy. The bar represents a length of 200 nm. The ceria particles are the small dark grains, with diameters between 5 and 10 nm. The particles are randomly distributed through the dispersion; this is consistent with SAXS results which show no preferred distances between them at this concentration

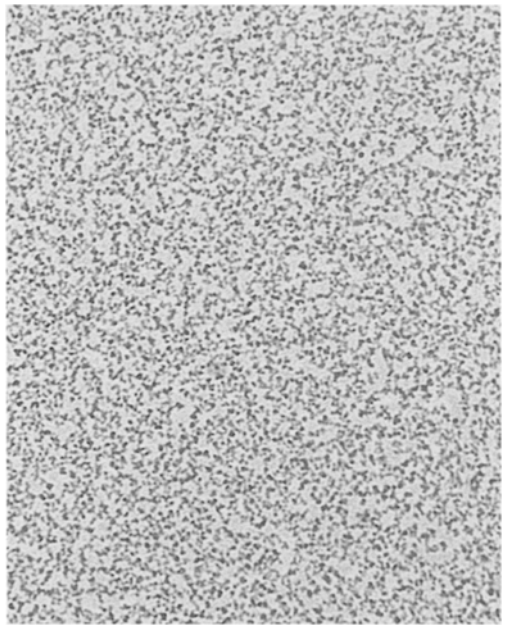

Fig. 10 Image of a dispersion containing 5 g/l ceria and 1 g/l PVP in aqueous HNO_3 at pH 2 obtained through cyo-transmission electron microscopy. The bar represents a length of 200 nm. The ceria particles are the small dark grains, with diameters between 5 and 10 nm. The ceria particles are collected into tenuous aggregates; this is caused by the formation of polymer bridges between the particles

distances between the particles at this concentration. The number density of particles is not significant, for 2 reasons: (i) the image is a projection of a 1000 Å thick film; (ii) the concentration of particles is increased during the blotting of excess liquid that procedes freezing.

Figure 10 presents an image of a dispersion containing ceria and PVP at 0.2 g of PVP per g of ceria. Here the particles are aggregated; again, the distance between the aggregates does not reflect the true distance between neighboring aggregates because the image reflects the structure of a dispersion at a higher concentration. The important feature is that the aggregates are quite tenuous: they have many rod-like sections, whereas random aggregates with a fractal dimension of 2 would appear opaque in a projection image. Also, these aggregates appear to form an extensive network throughout the dispersion: image taken in the thinner regions of the film show objects which are more tenuous (since fewer particles are projected) but not separated.

Discussion

Dispersions with two types of compositions have been studied in order to determine the influence of the polymer on the thermodynamic properties and structure of the dispersion. These two types of dispersions are discussed successively.

Dispersions with saturated surfaces

This condition is reached with 5 g of PVP per g of ceria. In this limit, the adsorbed polymers improve the stability of the dispersion; indeed, dispersions of pure ceria can be coagulated by adding salt; dispersions that are saturated with PVP require more added salt to reach macroscopic aggregation (Fig. 2). Consequently, we expect that the saturated dispersions should contain isolated particles covered with a few macromolecules each and coexisting with free macromolecules.

This expectation was checked through SAXS experiments. In dispersions made at 5 g of PVP per g of ceria, the particles were found to be independent, at all concentrations. The dispersions made at 2 g of PVP per g of ceria contained multiplets of ceria particles, with an average of 1.7 particle per multiplet; this aggregation number remained the same at all concentrations. Examination of the adsorption isotherm at 2 g/l indicated that the highest pseudo plateau was at 2.6 g/g. Thus, the samples at 2 g/g of PVP/CeO_2 were not completely saturated. Therefore the limited clustering observed at 2 g/g was caused by a compression in conditions where the surfaces were not completely saturated.

From this, we conclude that a complete saturation of the surface is necessary to protect the particles from aggregation under compression.

Dispersions with unsaturated surfaces

The chosen composition was 0.2 g of PVP per g of ceria, because around this composition the salt concentration needed to produce fast aggregation of ceria particles (ccc) is the lowest (Fig. 2).

In *dilute* ceria dispersions, osmotic pressure data show that there are *no permanent aggregates* of particles. On the other hand, the spatial organization of *concentrated dispersions* is remarkable, because it shows an *alternance of clusters and voids* at intermediate scales. Indeed, the SAXS curves show a peak at a position corresponding to distances significantly larger than the distances calculated from the number of particles in the dispersion volume (Fig. 8).

Another remarkable feature is that the peak position varies as the inverse of the concentration (Fig. 8). This unusual variation is expected for one-dimensional swelling of a lamellar system. However the electron microscopy

images do not show platelets nor flat aggregates. Instead, the ceria particles appear to form a mesh of random, tenuous and interpenetrated aggregates (Fig. 10). Therefore the data must be analyzed according to the swelling laws for dispersions of random aggregates.

For *permanent, interpenetrated aggregates* with a fractal dimension d_f, swelling in a three dimensional space, the swelling law depends on the difference $d - d_f$ only. Accordingly, the average distance ξ between the strands of neighboring aggregates may be predicted in units of the particle size a:

$$\xi/a = \phi^{-1/(d-d_f)} \tag{14}$$

If the fractal dimension is $d_f = 2$, as in the case of random polymers, then ξ must vary as ϕ^{-1}, as observed. Therefore the results can be analyzed as scattering from a space filling dispersion of permanent aggregates with fractal dimension $d_f = 2$. Similar types of organizations have been observed in dispersions [39] or emulsions [40] that have been aggregated through a diffusion limited mechanism.

However this model has two shortcomings. Firstly, the aggregates appear rather stringy through electron microscopy, whereas aggregates with $d_f = 2$ are opaque in a projection image. Secondly, osmotic pressure measurements in dilute solutions show that the aggregates dissociate at larger dilutions; therefore the dispersions are made of transient aggregates.

It is difficult to make predictions for *transient aggregates*, because their structures result from an equilibrium of binding and unbinding processes, which may themselves depend on the concentration of the dispersion. Computer simulations of polymer bridged aggregates have been performed by Dickinson [41]; they produce aggregates which look stringy and have fractal dimensions of the order of 1.7. Predictions of the interaggregate distance would be difficult to achieve, because of the very large number of particles which would be involved (however the model could be simplified by treating the polymers as spherical entities).

Another possibility is that the special one dimensional swelling that we observe could be the signature of a microphase separation as occurs with diblock systems [42–43] or mixtures of weakly charged polyelectrolytes [44–45]. Both systems can produce microdomains of lamellae which give a one-dimensional ordering relation. However, in order to have a microphase separation it is necessary to have a driving force. In our case it could be described as an interparticle potential which would be repulsive at large separations due to electrostatic repulsions and weakly attractive at short separations because of the polymer bridging.

In summary, the combination of polymer bridging and electrostatic repulsions causes changes in the spatial organization of the dispersions, with a one-dimensional alternance of clusters and voids. This unusual clustering is an intermediate state between the fully dispersed state and the macroscopically flocculated state.

Conclusion

Dispersions made of very small particles and very small adsorbing macromolecules are interesting because the energy of adsorption per macromolecule is weak; hence the organization of particles and macromolecules in the dispersion is ruled by the thermodynamic equilibrium. For polymer + colloid systems, this is quite unusual. Nevertheless, the general behavior remains classical, and in particular the adsorption of the polymer modifies the stability of the dispersion against an addition of salt. We were particularly interested in the equilibrium structures induced by the polymer adsorption and in the deswelling behavior in conditions where the stability was either depressed or enhanced by the polymer.

As the system is in equilibrium, many different ways can be used to concentrate a dispersion. In this work, we have used the osmotic stress method because the chemical potential of every small species can be adjusted to a desired value.

First, the reference case, pure ceria dispersion at pH 2, was examined. The main conclusions are threefold. In the dilute regime, the number average mass M_n was determined. In the concentrated regime, the osmotic pressure is very high and arises entirely from electrostatic interactions. In the concentrated regime again, the particles order in a three-dimensional array. None of these results are really surprising but the main success of this part of the work was to demonstrate the quantitative agreement between the experimental pressure and the electrostatic pressure. A puzzling result remains that the pressure is not changed by a partial aggregation of the system.

A second set of conclusions can be drawn from the study of ceria dispersions that are saturated with PVP. In the dilute regime, the stability against the salt addition is improved. In the concentrated regime, the particles retain their three-dimensional short range order, but the resistance against osmotic deswelling is much higher than in pure ceria dispersions. Thus, our conclusion is that short macromolecules achieve properly their role of bumpers between the particles in concentrated regime but at the excessive cost of a very high osmotic resistance against deswelling. In that respect, they are not good additives if both stability in the concentrated regime and easy deswelling are required.

This resistance against deswelling is unavoidable with weakly adsorbed macromolecules, for two reasons. First,

the adsorbed layers are not compressed by the adsorption. Second, there is a high concentration of free polymer in the solution. Indeed, we have demonstrated that the osmotic pressure of saturated dispersions matches that of polymer solutions containing the same amount of polymer. Therefore, in order to achieve a good protection of nanometric particles without the cost of extra osmotic pressure, it is absolutely necessary to use small species which are strongly adsorbed or grafted on the particle surfaces.

Finally, when the polymer does not saturate the surfaces, the particles may associate to share the available macromolecules. The bridging may be promoted by the addition of salt or by a compression of the dispersion. Addition of salt to unsaturated dispersions causes macroscopic flocculation at ionic strengths where the pure dispersions are still stable. Compression of unsaturated dispersions causes limited aggregation but no macroscopic phase separation. The organization of the compressed dispersions is unusual: it shows an alternance of clusters and voids, and the separations of clusters show a one-dimensional swelling when the water content of the dispersion is varied. This unusual organization results from a competition of long range electrostatic repulsions and shorter range bridging attractions. Since this type of competition is not uncommon in colloidal systems, it follows that such microsphase separated structures may occur more frequently than it was previously realized.

Acknowledgment We thank Luc Belloni for his guidance on PB calculations, Cécile Bonnet-Gonnet and Cécile Roselli who kindly allowed us to use their unpublished work on osmotic pressure of dextran solutions (Eqs. (3, 4), Gabriel Schreyek for his contribution to the initial stage of this work, Patricia Lixon for all the SEC measurements and Michel Delsanti for useful discussions.

References

1. Lyklema J (1968) Adv Colloid Interface Sci 2:65
2. Fleer GJ, Lyklema J (1974) J Colloid Interface Sci 46:1
3. Vincent B (1974) Adv Colloid Interface Sci 4:193
4. Pelssers EGM, Cohen Stuart MA, Fleer GJ (1989) Colloids Surfaces 38:15
5. Cabane B, Wong K, Wang TK, Lafuma F (1988) Colloid Polym Sci 266:101
6. Wong K, Cabane B, Duplessix R (1988) J Colloid Interface Sci 123:466
7. Lafuma F, Wong K, Cabane B (1991) J Colloid Interface Sci 143:9
8. Wong K, Lixon P, Lafuma F, Lindner P, Aguerre Charriol O, Cabane B (1992) J Colloid Interface Sci 153:55
9. Spalla O, Cabane B (1993) Colloid Polym Sci 271:357
10. Spalla O, Cabane B (1993) in: "Colloid-Polymer Interactions", ACS Symposium Series 532:35, Dubin P and Tong P eds, ACS, Washington, DC
11. Klein J, Luckham P (1984) Nature 308:836
    Almog, Klein J (1985) J Colloid Interface Sci 106:33
12. Cosgrove T (1990) J Chem Soc Faraday Trans 86:1323
13. Cosgrove T, Crowley TL, Ryan K, Webster JRP (1990) Colloids Surfaces 51:255
14. Auvray L, Cotton JP (1987) Macromolecules 20:202
15. Scheutjens JMHM, Fleer GJ (1985) Macromolecules 18:1882
16. Chane-Ching JY (1987) European Patent EP 208580
17. Wong K, Aguerre Charriol O, Cabane B, unpublished work
18. Nabavi M, Spalla O, Cabane B (1993) J Colloid Interface Sci 160:459
19. de Gennes PG (1979) Scaling Concept in Polymer Physics, Cornell University Press, New York
20. Cohen-Stuart MA (1980) Phd thesis, Wageningen, Netherland
21. Parsegian VA, Rand RP, Fuller NL (1979) Proc Natl Acad Sci 76(6):2750
22. Rohrsetzer S, Kovacs P, Nagy M (1986) Colloid Polymer Science 264:812
23. Parsegian VA, Rand RP, Fuller NL, Rau DC (1986) Methods in Enzymol 127:400
24. Taylor KA, Glaeser RM (1976) J Ultrastruct Res 55:448
    Dubochet J, Adrian M, Chang J, Homo JC, Lepault J, Mc Dowall AW, Schultz P (1988) Quaterly Review of Biophysics 21:2
25. Bellare JR, Davis HT, Scriven LE, Talmon Y (1988) J Electron Microsc Tech 10:87
26. Clausen TM, Vinson PK, Minter JR, Davis HT, Talmon T, Miller WG (1992) J Phys Chem 96:474
27. Cochin D, Candau F, Zana R, Talmon Y (1992) Macromolecules 25:4220
28. Laughlin RG, Munyon RL, Burns JL, Talmon Y (1992) J Phys Chem 96:474
29. Kamenka N, Chorro M, Talmon Y, Zana R (1992) Colloids Surfaces 67:213
30. Dubuisson JM, Dauvergne JM, Depautex C, Vachette P, Williams CE (1986) Nucl Inst Methods Phys Res A246:636
31. Hayter JB, Penfold J (1981) Molecular Phys 42:109
32. Hansen JP, McDonald IR (1976) Theory of simple liquids, Academic Press
33. Cebula DJ, Goodwin JW, Jeffrey GC, Ottewill RH, Parentich A, Richardson RA (1983) Faraday Discuss Chem Soc 76:37
34. Cohen-Stuart MA, Scheutjens JMHM, Fleer GJ (1980) J Polym Sci 18:559
35. Napper DH (1983) Polymeric Stabilization of Colloidal Dispersions, Academic Press, New York
36. Verwey EJW, Overbeek JTG (1948) Theory of the Stability of Lyophobic Colloids, Elsevier Amsterdam
37. Belloni L, Drifford M, Turq P (1984) Chem Phys 83:147
38. Bonnet-Gonnet C, Belloni L, Cabane B (1994) Langmuir 10:4012
39. Carpineti M, Giglio M (1992) Phys Rev Lett 68:3327
40. Bibette J, Mason TG, Hu Gang, Weitz DA (1992) Phys Rev Lett 69:981
41. Dickinson E, Euston SR (1991) J Chem Soc Faraday Trans 87:2193
42. Leibler L (1980) Macromolecules 13: 1602
43. Helfand E, Wasserman Z (1982) Chap 4 in Developments in Block Co-polymers-1, Edited by I. Goodman, Applied Science, New York
44. Khlokhlov AR, Nyrkova IA (1992) Macromolecules 25:1493
45. Nyrkova IA, Khlokhlov AR, Doi M (1993) Macromolecules 26:3601